

Ethylation of ethylbenzene with ethanol over substituted medium pore aluminophosphate-based molecular sieves

B. Rajesh^a, M. Palanichamy^a, V. Kazansky^b, V. Murugesan^{a,*}

^a Department of Chemistry, Anna University, Chennai 600025, India

^b Zelinsky Institute of Organic Chemistry, Leninsky Prospect, Moscow, Russia

Received 10 November 2001; received in revised form 21 February 2002; accepted 23 April 2002

Abstract

Medium pore aluminophosphate-based molecular sieves like AIPO-41, CoAPO-41, CoAPSO-41 and MnAPSO-41 have been synthesised hydrothermally using dipropylamine as the organic template. These materials have been characterised by various physical methods including X-ray powder diffraction (XRD), thermogravimetric analyses (TGA), FT-IR, ESR and scanning electron microscope (SEM). All these materials are found to be crystalline and do not contain any detectable impure phases. The catalytic performance of these materials has been examined for ethylation of ethylbenzene with ethanol at 250, 300, 350, 400 and 450 °C. Ethylbenzene conversion is observed to increase with increase in temperature with the maximum conversion at 400 °C. The major product is 1,4-diethylbenzene whose selectivity decreases with increase in temperature over all the catalysts. High temperature is favourable for the formation of 1,3-diethylbenzene which is thermodynamically more stable than the other products. Influence of feed ratio on conversion and products selectivity is examined and the results are discussed in this paper.

© 2002 Elsevier Science B.V. All rights reserved.

Keywords: Medium pore; AIPOs; Characterisation; Ethylation; 1,4-Diethylbenzene

1. Introduction

Medium pore AIPO-41 was first synthesised by Lesch and Wilson [1] as a mixed phase. Later Clark et al. [2] reported the possibility of obtaining AIPO-41 as a pure phase using mixed alcohol/water solvent system. However, the synthesis procedure required numerous steps and relatively long crystallisation time. The AFO framework topology consists of elliptical uni-dimensional 10 ring channels that are slightly larger than the 10 ring channels in the AEL structure type [3]. This structure type -41 is less

widely studied medium pore molecular sieve. Transition metal incorporated aluminophosphate molecular sieves have gained considerable significance during the last several years mainly due to the bi-functional characteristics of these materials in several catalytic reactions [4]. Si and Mn substitution in the AFO framework has been reported by Prakash et al. [5]. Ni and Co substitution in the AFO framework is reported by Hartmann et al. [6]. Medium pore zeolites are well known for their catalytic activity and shape selective feature in acid-catalysed reactions such as alkylation of aromatics [7], isomerisation of alkylaromatics [8] and methanol conversion [9]. However, studies of these reactions using medium pore AIPO-41 based molecular sieves are scanty.

* Corresponding author. Tel.: +91-44-2200660;

fax: +91-44-2200660.

E-mail address: v_murugu@hotmail.com (V. Murugesan).

The catalytic activity of silicon incorporated AIPO-41 based molecular sieve is found to be high due to the relatively large amount of Brönsted acid sites created by the substitution of silicon in the framework of phosphorus sites. In continuation of our work in this area, we report herein the synthesis of AIPO-41, CoAPO-41, CoAPSO-41 and MnAPSO-41 and their characterisation by X-ray powder diffraction (XRD), thermogravimetric analyses (TGA), FT-IR, ESR and scanning electron microscope (SEM). The catalytic performance of these materials has been examined towards ethylation of ethylbenzene in the vapour phase. The interest in this particular reaction lies in the fact that one of the isomeric products, namely, 1,4-diethylbenzene is the raw material for the production of 1,4-divinyl benzene which is used in the manufacture of cross-linked styrene. The reaction has been studied at different temperatures and the influence of feed ratio on conversion and product selectivity is also examined.

2. Experimental

2.1. Synthesis

AIPO-41, CoAPO-41, CoAPSO-41 and MnAPSO-41 have been synthesised hydrothermally using dipropylamine as the organic template. The following chemicals were used without further purification: orthophosphoric acid (88%, Merck), aluminium hydroxide (Merck), dipropylamine (99%, Acros), tetraethyl orthosilicate (Merck), cobalt(II)acetate (Merck) and manganese acetate (SRL). Synthesis were carried out in 300 ml stainless steel autoclaves at autogeneous pressure without agitation. The molar compositions of the synthesis gels were:

AIPO-41 0.7Al₂O₃ : 1.0P₂O₅ : 4Pr₂NH : 48H₂O

CoAPO-41 0.3CoO : 0.98Al₂O₃ : 1.25P₂O₅
: 4Pr₂NH : 55H₂O

CoAPSO-41 0.3CoO : 0.98Al₂O₃ : 0.1SiO₂
: 1.25P₂O₅ : 4Pr₂NH : 55H₂O

MnAPSO-41 0.1MnO : 0.98Al₂O₃ : 0.1SiO₂
: 1.25P₂O₅ : 4Pr₂NH : 55H₂O

In a typical synthesis of AIPO-41, aluminium hydroxide (7.64 g) was slowly added to a solution containing 7.2 ml orthophosphoric acid in 35 ml water. The mixture was stirred for 3–4 h until a homogeneous gel was obtained. Dipropylamine was then added dropwise and stirring was maintained for another 2 h. AIPO-41 crystals were obtained when the gel was autoclaved at 473 K for 15 h. In the preparation of CoAPO-41, CoAPSO-41 and MnAPSO-41 corresponding acetate salts of cobalt, manganese and tetraethyl orthosilicate of sufficient quantities were added to the aluminophosphate gel prepared as described above prior to the addition of dipropylamine. The crystallisation of CoAPO-41, CoAPSO-41 and MnAPSO-41 was obtained when the gels were autoclaved at 473 K for 24 h. The solid products obtained

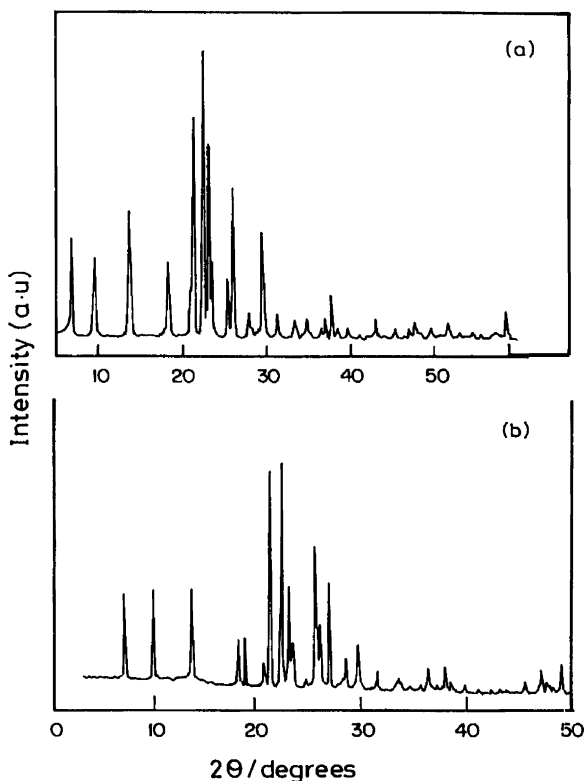


Fig. 1. The XRD patterns of: (a) AIPO-41 and (b) MnAPSO-41.

were filtered, washed several times with deionised water and air-dried. The samples were calcined at 550 °C for 6 h in the presence of air before the reaction was carried out.

2.2. Characterisation

The XRD patterns were recorded on a Rigaku miniflex diffractometer using Cu K α radiation in the scan range of $2\theta = 5$ to 50°. TGA were carried out on a Mettler 2000 thermal analyser at a heating rate of 15 °C/min. FT-IR spectra of the samples were recorded using Nicolet Avatar 360 spectrometer. Electronic absorption spectra were recorded on a Perkin-Elmer 330 UV–VIS spectrophotometer using quartz as the reference sample. The morphology of the materials was tested by Philips ESEM with TMP + EDAX SEM.

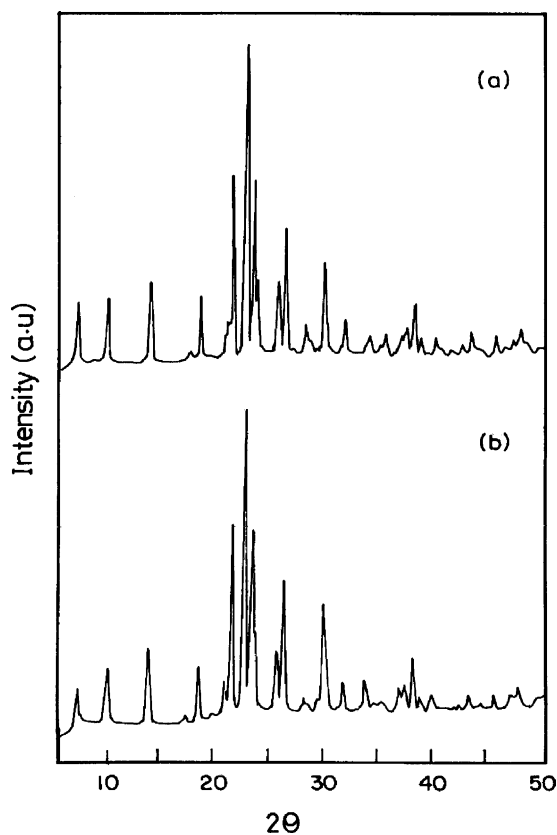


Fig. 2. The XRD patterns of: (a) CoAPO-41 and (b) CoAPSO-41.

2.3. Catalytic studies

The reactor system was a fixed-bed, vertical, flow type reactor made up of glass tube of 40 cm length and 2 cm i.d. The glass reactor was heated to the requisite temperature with the help of a tubular furnace controlled by a digital temperature controller cum indicator. About 2 g of the catalyst was placed in the middle of the reactor and supported on either side with a thin layer of quartz wool and ceramic beads. The reactants were fed into the reactor by a syringe infusion pump that could be operated at different flow rates. The reaction was carried out at atmospheric pressure. The products were passed through a water-cooled condenser attached to the end of the reactor. The liquid products collected for the first 15 min were discarded

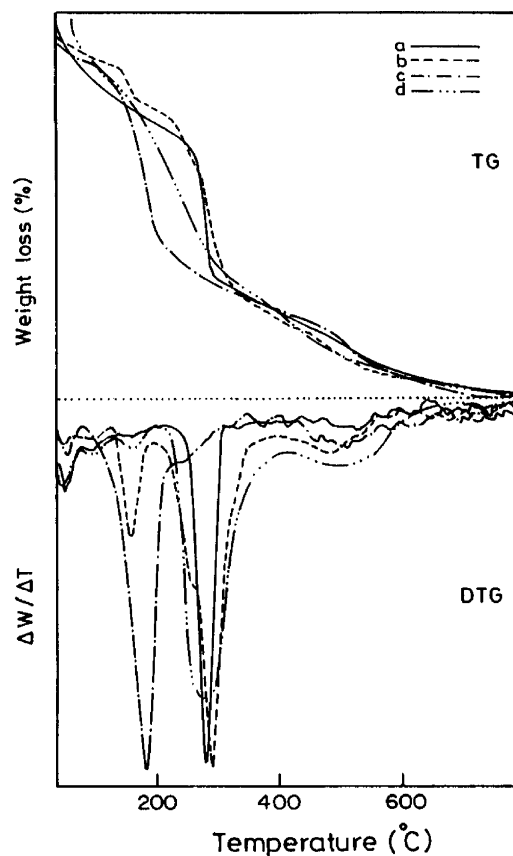


Fig. 3. The TG and DTG curves of: (a) AlPO-41, (b) CoAPO-41, (c) CoAPSO-41 and (d) MnAPSO-41.

and analysis was made only with the products collected after this time. This has been done to ensure the attainment of steady state for the reaction over the catalyst and also to eliminate temperature fluctuations. After each run, the catalyst was heated at 500 °C for regeneration in order to remove the deposited coke.

3. Results and discussions

3.1. Characterisation

The XRD patterns of the as synthesised AlPO-41, MnAPSO-41, CoAPO-41 and CoAPSO-41 (Figs. 1 and 2) show that the materials are highly crystalline

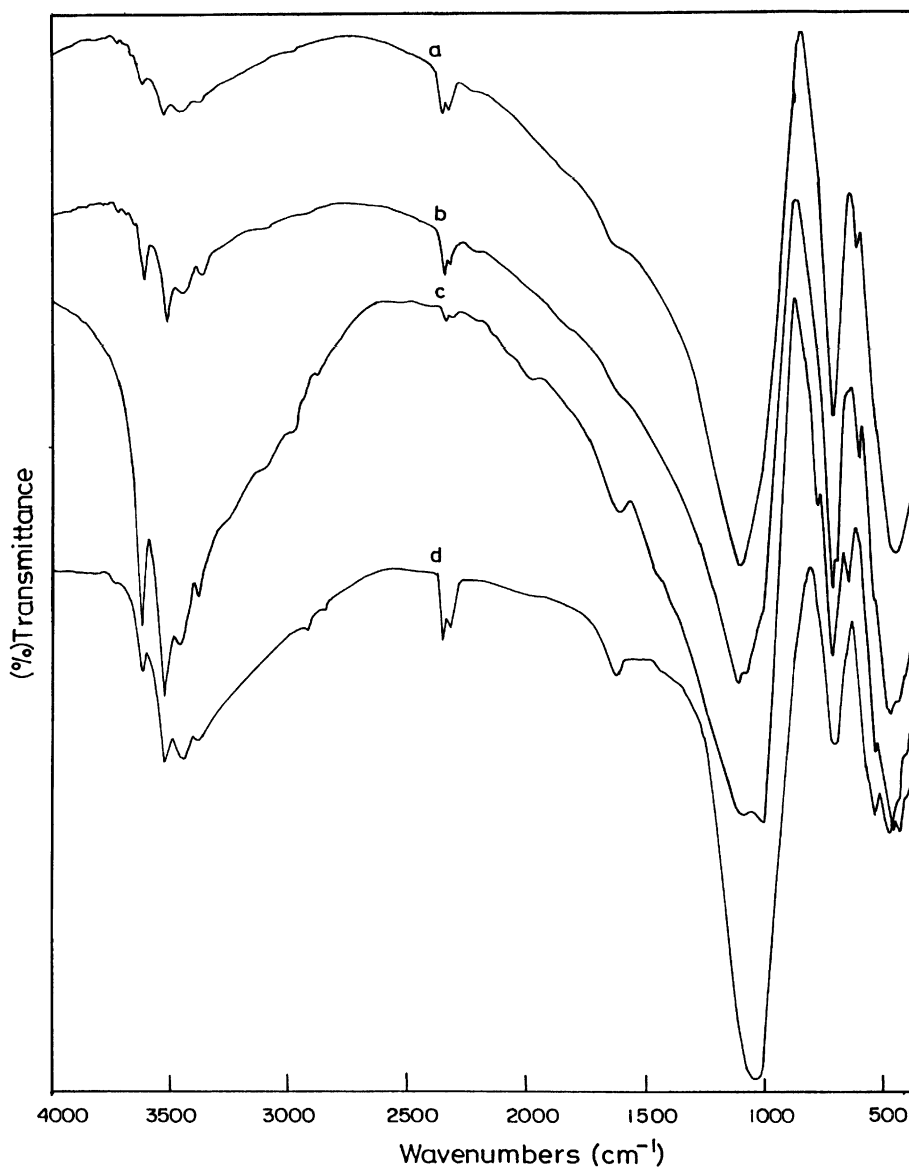


Fig. 4. FT-IR spectra of: (a) AlPO-41, (b) CoAPO-41, (c) CoAPSO-41 and (d) MnAPSO-41.

and do not contain detectable impure phases. The thermal properties of the various AFO compositional variants have been investigated by TGA (Fig. 3). The initial weight loss up to 400 K is due to the desorption of physically adsorbed water. The desorption of the organic template takes place in a single-step in AlPO-41 and in multi-steps in other materials. The low temperature weight loss around 570 K in all the compositional variants is tentatively assigned to the decomposition of dipropylamine occluded inside the channels. The high temperature weight loss around 770 K is assigned to the desorption and decomposition of protonated amines balancing the framework negative charge. The FT-IR spectra of the samples (Fig. 4) show a peak at 3451.89 cm^{-1} due to hydroxyl ($-\text{OH}$) stretching of water. It is confirmed by its bending mode at 1639.26 cm^{-1} . The peak at 3523.67 cm^{-1}

is due to the bridging $-\text{OH}$ stretching. The terminal $\text{P}-\text{O}-\text{H}$ stretching is observed at 3619.73 cm^{-1} . The locked in template is evident by its $\text{C}-\text{H}$ stretching at 2924.61 cm^{-1} . The overtone band at 2310.61 cm^{-1} is due to the combination of framework asymmetric (1029.67 cm^{-1}) and symmetric (729.90 cm^{-1}) modes.

The ESR spectra of CoAPO-41, CoAPSO-41 and MnAPSO-41 are as shown in Fig. 5. The signals in each spectrum are broad without clear hyperfine splitting illustrating significant metal d-electron delocalisation over the framework. The g -value is calculated to be 3.1706 for CoAPO-41 and the spectrum clearly indicates the presence of only one species. Hence, cobalt(II) is suggested to be placed exclusively in the framework. The g -value of CoAPSO-41 is found to be 3.3687. This value is slightly higher than that of CoAPO-41 and this difference could be attributed to

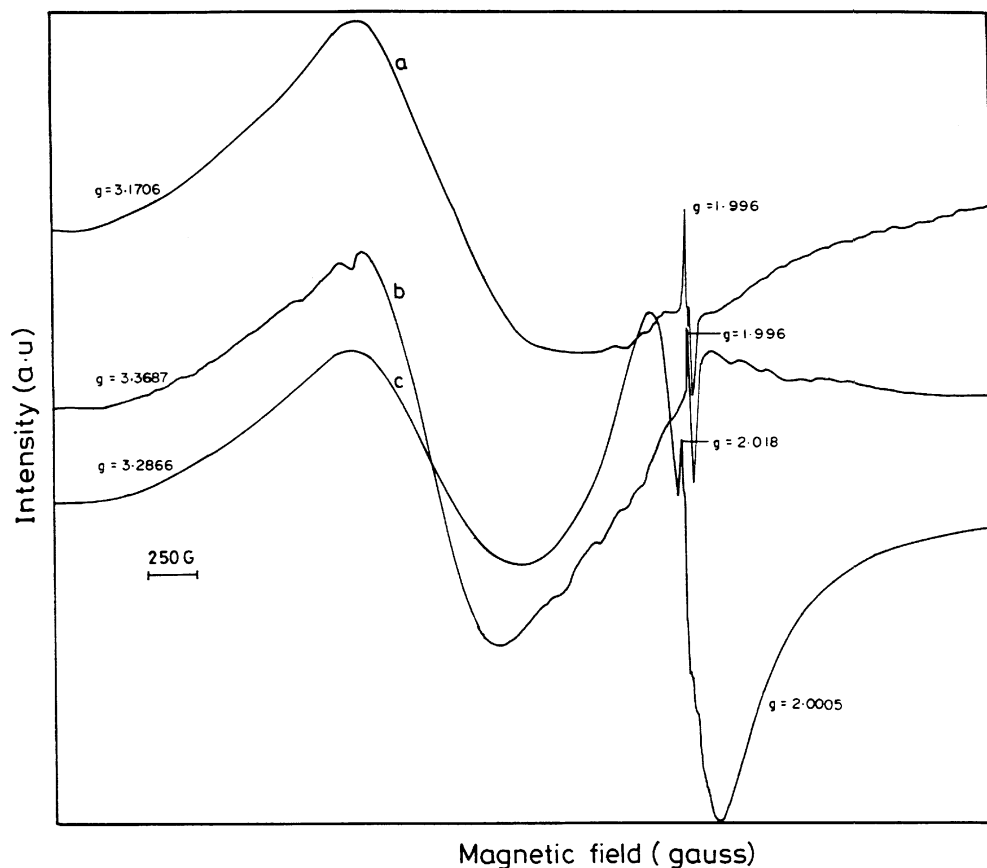


Fig. 5. ESR spectra of: (a) CoAPO-41, (b) CoAPSO-41 and (c) MnAPSO-41.

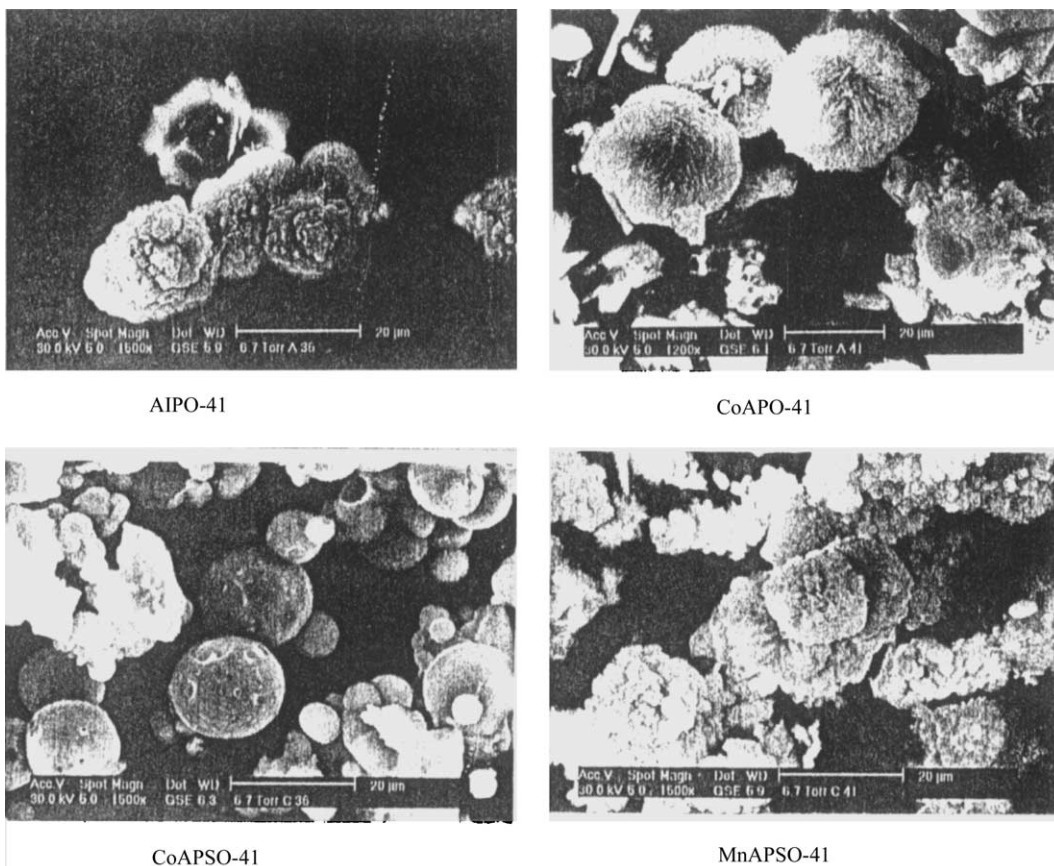


Fig. 6. The SEM pictures of: (a) AIPO-41, (b) CoAPO-41, (c) CoAPSO-41 and (d) MnAPSO-41.

Si in the framework which can enhance the metal electron delocalisation. Two g -values are observed for MnAPSO-41 in its spectrum. The first one with $g = 3.2866$ is assigned to Mn(II) in the framework and the second one with $g = 2.0005$ is assigned to either non-framework Mn(II) or organic free radical formed during calcination as reported earlier [5]. This calculation is based on the high intensity of the signal in the present spectrum compared to the intensity of the signal reported in the literature [5]. The SEM pictures of AIPO-41, CoAPO-41, CoAPSO-41 and MnAPSO-41 are as shown in Fig. 6a–d. The micrographs are found to be polycrystalline aggregates of nearly spherical morphology, and more so in CoAPO-41 and CoAPSO-41. Each tiny crystal in every aggregate is thread like and this nature of parent

AIPO-41 is maintained in other three materials. Similar morphology for SAPO-41 is reported earlier [10].

3.2. Ethylation of ethylbenzene

Ethylation of ethylbenzene with ethanol was carried over all the catalysts at 250, 300, 350, 400 and 450 °C. The feed ratio of ethylbenzene:ethanol is 1:1. The major products are 1,2-, 1,3- and 1,4-diethylbenzene. The ethylbenzene conversion and products selectivity are illustrated in the Figs. 7 and 8. The conversion increases with increase in temperature over all the catalysts and attains maximum at 400 °C. Beyond this temperature, the conversion decreases as a result of coke deposition. The selectivity to-

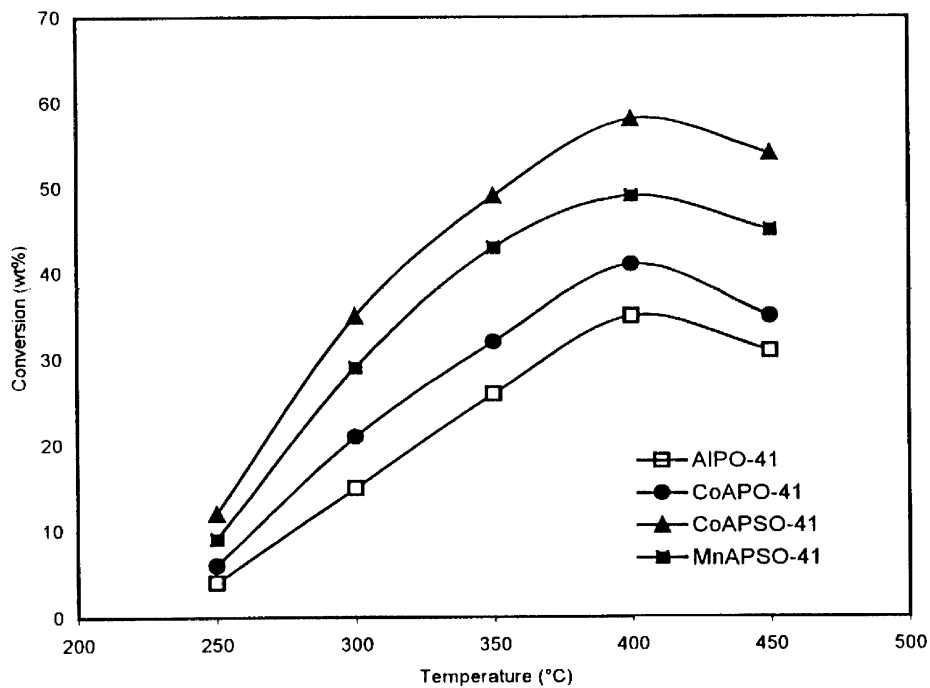


Fig. 7. The effect of temperature on ethylbenzene conversion.

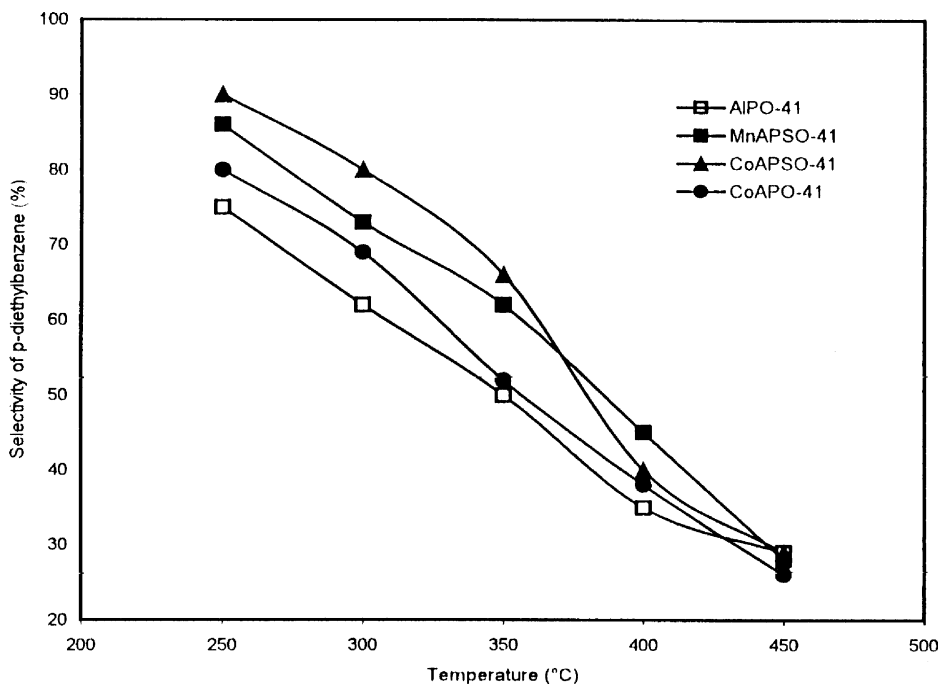


Fig. 8. The effect of temperature on products selectivity.

wards 1,4-diethylbenzene decreases beyond 400 °C, whereas, 1,2- and 1,3-diethylbenzene selectivity increases. Since, AlPO molecular sieves are largely hydrophobic, the adsorption of ethylbenzene on the Brønsted acid sites in addition to ethanol is unavoidable. This adsorption is the root cause for the formation of 1,3-diethylbenzene as reported in the literature [11]. At lower temperature, most of the ethylbenzene is in the vapour state without much adsorption. Hence, when ethylbenzene in the vapour state approaches the layer of ethyl cations on the channel surface, it can better use its *para* position for electrophilic attack to produce 1,4-diethylbenzene, as its *ortho* position offers little steric hindrance and the *meta* position demands high activation energy for electrophilic attack. Hence, selectivity to 1,4-diethylbenzene is high at lower temperature.

With increase in temperature, adsorption of ethylbenzene on the Brønsted acid sites is expected to increase particularly in the *para* position as it has more electron density. This results in *ortho* and *meta* positions favourable for electrophilic attack. So, the substitution at these positions increases with increase in temperature. Even if adsorption occurs on one of the *ortho* positions of ethylbenzene, the other *ortho* position could be used for electrophilic attack. Again adsorption of this kind could also help in bringing ethylbenzene close to any adsorbed ethyl cation, thus,

giving little increment in 1,2-diethylbenzene selectivity with increase in temperature. Although AlPO-41 is electrically neutral with avoidance of acidity, the presence of mild acid sites is due to crystal imperfections as evident from ethylbenzene conversion. Similar increase in conversion is also observed for CoAPO-41, CoAPSO-41 and MnAPSO-41 molecular sieves.

At 400 °C, the trend of conversion lies in the order CoAPSO-41 > MnAPSO-41 > CoAPO-41 > AlPO-41. This order is based on the density of acid sites generated by isomorphous substitution. Isomorphous substitution is more in CoAPSO-41 than in MnAPSO-41 which is partly evident from the intensity of bridged –OH stretching absorption in the FT-IR spectrum as shown in Fig. 4. More isomorphous substitution of Co(II) than Mn(II) in the framework derives the driving force from crystal field stabilisation. There is no crystal field stabilisation for Mn(II) as it has d^5 electronic configuration, whereas, Co(II) acquires it as it has $3d^7$ electronic configuration [12].

Since, conversion is maximum at 400 °C over all the catalysts, it was decided to study the influence of feed ratio (ethylbenzene:ethanol) at 1:2 and 1:3 on conversion at this temperature. The results are illustrated as shown in Figs. 9 and 10. Conversion decreases with increase in ethanol content in the feed. Increase in ethanol content in the feed could dilute ethylbenzene in the vapour phase, thus, reducing its reaction

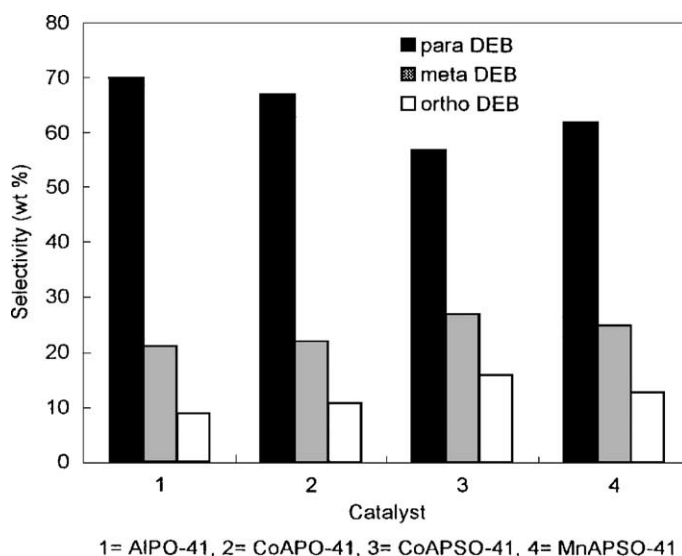


Fig. 9. Products selectivity for ethylbenzene:ethanol = 1:2.

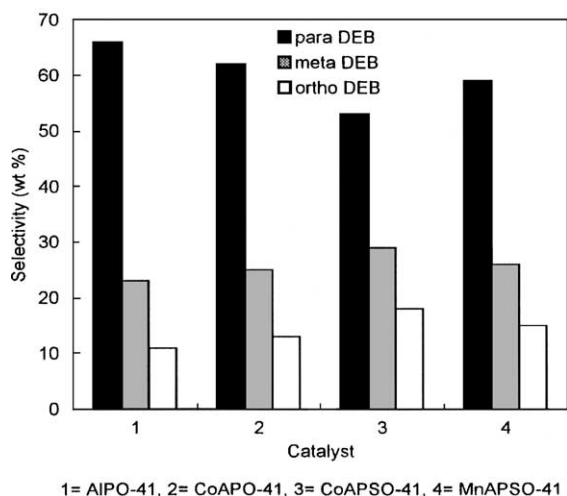


Fig. 10. Products selectivity for ethylbenzene:ethanol = 1:3.

with ethyl cation adsorbed on the Brönsted acid sites of the catalysts. In addition, adsorption of ethylbenzene on the Brönsted acid sites is also reduced. This decrease in adsorption of ethylbenzene explains why the increase in selectivity to 1,3-diethylbenzene is not as high as in the feed ratio 1:1. Like the decrease in the selectivity to 1,4-diethylbenzene, the selectivity to 1,2-diethylbenzene might also decrease. With increase in the feed ratio, the ethyl cation content on the surface of the catalyst will increase. This would facilitate diffusion of ethylbenzene in the vapour state with its ethyl group very close to ethyl cation due to van der Waal's force. Hence, it could contribute to little increment to *ortho* substitution. Although at the *ortho* position there is steric hindrance, increase in temperature is more beneficial to *ortho* substitution and at the given temperature, increase in ethanol content in the feed could also increase the *ortho* substitution.

4. Conclusion

Hydrothermal synthesis of AlPO-41, CoAPO-41, CoAPSO-41 and MnAPSO-41 has been achieved using dipropylamine as the structure-directing agent. Synthesis parameters for the preparation of pure and highly crystalline samples have been optimised. The characterisation by physico-chemical methods revealed the phase purity, crystallinity, morphology

and thermal stability of the materials. The density of Brönsted acid sites increases in the order AlPO-41 < MnAPSO-41 < CoAPO-41 < CoAPSO-41 as evidenced from the FT-IR spectra of the samples, based on the intensity of bridged –OH stretching. The same order is also observed for the density of terminal –OH groups. The signals in ESR spectra of the samples were broad without clear hyperfine splitting illustrating significant metal d-electron delocalisation over the framework. The SEM pictures clearly indicate the polycrystalline aggregates of nearly spherical morphology for all the materials. 1,4-Diethylbenzene has been found to be the major product in the ethylation of ethylbenzene reaction at low temperatures while the *meta* isomer predominates at higher temperatures.

Acknowledgements

The authors gratefully acknowledge the Department of Science and Technology, New Delhi for their financial support in carrying out this work through a sponsored research project under the Integrated Long Term Programme (ILTP) between India and Russia. One of the authors (B. Rajesh) is thankful to DST for the award of Project Associate.

References

- [1] D.A. Lesch, S.T. Wilson, Eur. Pat. Appl. (1988) 254075.
- [2] H.W. Clark, W.J. Rievert, M.M. Olken, Microporous Mater. 6 (1996) 115.
- [3] R.M. Kirchner, J.M. Bennett, Zeolites 14 (1994) 523.
- [4] J.C. Vedrine, Zeolite chemistry and catalysis, In: P.A. Jacobs, N.I. Jaeger, L. Kubelkova, B. Wichterlova (Eds.), Studies in Surface Science and Catalysis, Vol. 69, Elsevier, Amsterdam, 1991, p. 25.
- [5] M. Prakash, M. Hartmann, L. Kevan, J. Phys. Chem. B 101 (1997) 6819.
- [6] M. Hartmann, A.M. Prakash, L. Kevan, J. Chem. Soc. Faradays Trans. 94 (5) (1998) 723.
- [7] W.W. Kaeding, C. Chu, L.B. Young, B. Weinstein, S.A. Butter, J. Catal. 67 (1981) 159.
- [8] L.B. Young, S.A. Butter, W.W. Kaeding, J. Catal. 76 (1982) 418.
- [9] D. Chang, A.J. Silvestri, J. Catal. 47 (1977) 249.
- [10] P. Meriaudeau, V.A. Tuan, V.T. Naghiem, S.Y. Lai, L.N. Hung, C. Naccache, J. Catal. 169 (1997) 55.
- [11] C. Kannan, S.P. Elangovan, M. Palanichamy, V. Murugesan, Indian J. Chem. Tech. 5 (1988) 65.
- [12] A. Cotton, G. Wilkinson, Advanced Inorganic Chemistry—A Comprehensive Text, Wiley, New York, 1999.